Dilepton Distributions at Backward Rapidities

M. B. Gay Ducati
beatriz.gay@ufrgs.br

High Energy Phenomenology Group
Instituto de Física
Universidade Federal do Rio Grande do Sul
Porto Alegre, Brazil

GFPAE - UFRGS
http://www.if.ufrgs.br/gfpae

Talk based on works Phys. Lett. B 636, 46 (2006) and hep-ph/0607247.

Outline

- Motivation;
- High Density System
- Forward rapidities;
  - Color Glass Condensate;
  - Saturation effects;
  - p_T and rapidity distributions;
  - Cronin data on hadron production at forward rapidities.
- Backward rapidities;
  - Dipole approach;
  - nuclear effects at small and large Bjorken x;
  - p_T and rapidity distributions;
  - Cronin data on hadron production at backward rapidities.
- Conclusions.

Motivation

- Dilepton ⇒ Clean probe (eletromagnetic interactions);
- Forward rapidities:
  - RHIC and LHC experiments are characterized by a high density of gluons in the nucleus;
  - Those interactions can be described by dense condensates (Color Glass Condensates);
  - Search for signatures of the CGC description of the saturated regime;
  - Cronin peak suppression at forward rapidities for hadrons ⇒ Initial/Final state effect?
  - Dilepton ⇒ presenting the same suppression (Cronin peak suppression for hadrons ⇒ Initial state effect)
- Backward rapidites:
  - Nucleus at large Bjorken x;
  - Information about large x nuclear effects;
  - Pronounced Cronin peak at backward rapidities for hadrons ⇒ Initial/Final state effect?
  - Dilepton ⇒ which is the behavior at backward??

Partonic System Evolution

- Parton at large Bjorken $x \Rightarrow$ Valence quarks.
- Increasing energy $\Rightarrow$ Sea quarks.
- New partons are emitted.
- Emission probability $\propto \alpha_s \ln\left(\frac{1}{x}\right)$.
- DGLAP and BFKL evolution (only emission diagrams).
- At small x region (high energy limit).
- Density of partons increases.
- Large occupation number (partons eventually overlap).
- Recombination processes (GLR, AGL, BK, JIMWLK).

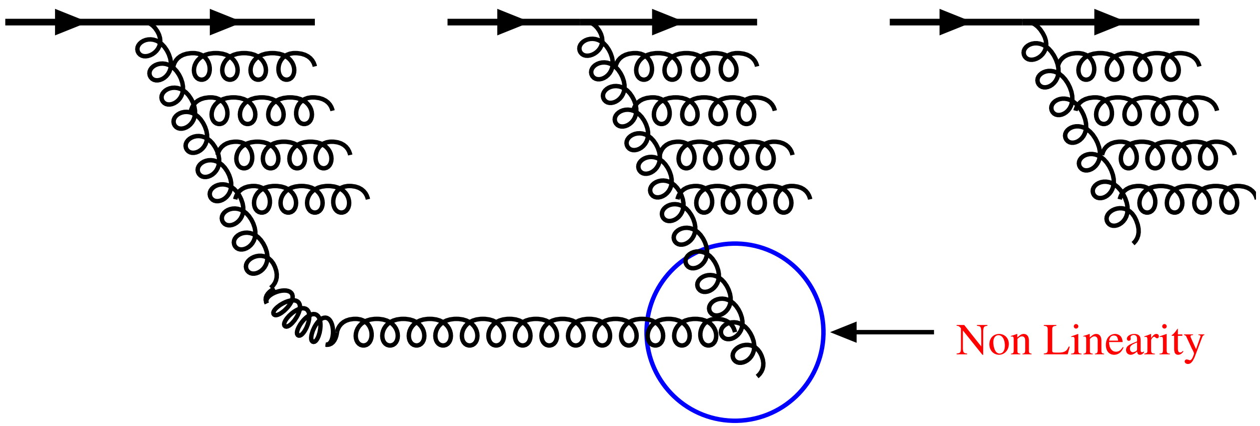

- Gluon dominance at small x.

Partonic System Evolution

- DGLAP and BFKL
- Consider only emission diagrams
- DGLAP $\rightarrow$ evolution in Q^2 ($\rightarrow$ diluted system)
- BFKL $\rightarrow$ evolution in x. ($\rightarrow$ saturation)
- Saturation $\rightarrow$ overlap in phase-space (small x and low Q^2).

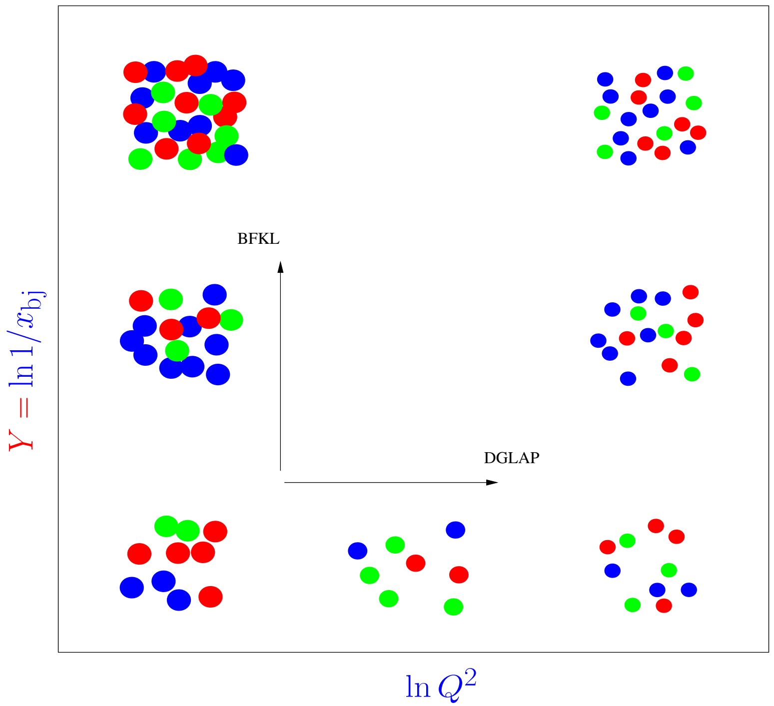

- High density system picture

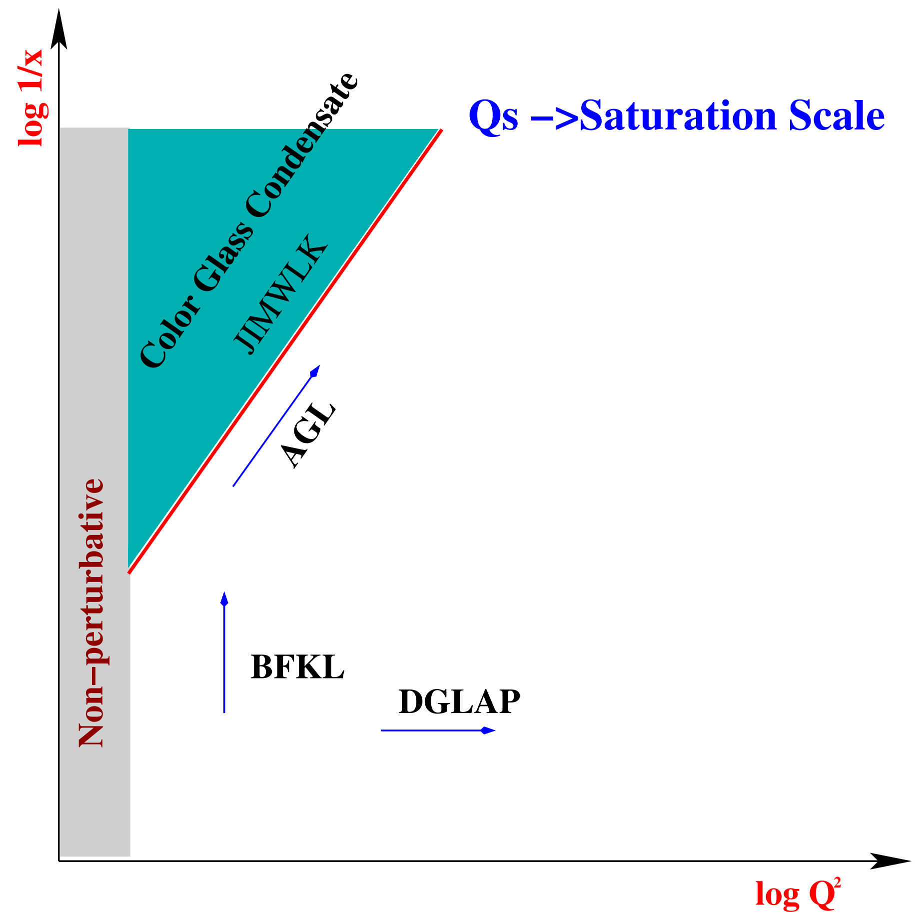

Color Glass Condensate (CGC)

L. McLerran, R. Venugopalan (1994)

Developped to describe the nucleus at high energy limit.

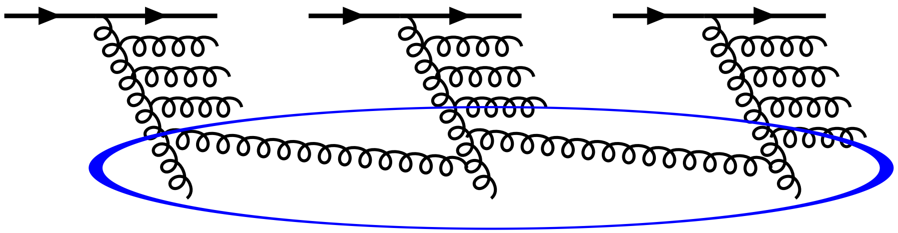

Small x Gluons

- Color $\Rightarrow$ Gluonic field dominance at small x.
- Glass $\Rightarrow$ Internal dynamics evolves slowly compared with the typical interaction scale time.
- Condensate $\Rightarrow$ Dense and saturated gluonic field.

The theory:

- Separation of small x and large x modes.
- Small x modes $\Rightarrow$ large occupation number
  - Described by classical color field $\mathcal{A}^{\mu}$ (CGC)
- Large x modes $\Rightarrow$ acts as sources of the small x modes
  - Described by frozen color sources ρ_a

Color Glass Condensate

- $\mathcal{A}^\mu$ obeys classical Yang-Mills's equations

$$[D_{\mu\nu}, F_a^{\mu\nu}] = \delta^{\mu +} \rho_a(x^-, x_\perp)$$

- $\rho_a(x, x_\perp)$ stochastic variable with zero expectation value.
- average over all ρ_a configurations, with the gauge-invariant weight functional $\mathcal{W}_{\Lambda^+}[\rho_a]$
- $\mathcal{W}_{\Lambda^+}[\rho_a]$ driven by JIMWLK evolution equation.
- $p^+ > \Lambda^+$ fast gluons, $p^+ < \Lambda^+$ soft gluons.
- Observables are calculated by averaging over the sources configurations by means of

$$\langle A_a^i(x^+, \vec{x}) A_b^j(x^+, \vec{y}) ... \rangle_{\Lambda^+} = \int \mathcal{D}_\rho \mathcal{W}_{\Lambda^+}[\rho] \mathcal{A}_a^i(\vec{x}) \mathcal{A}_b^j(\vec{y}).$$

Phenomenology:

- The color source distribution employed here is a Non-local Gaussian (predicted by the mean field asymptotic solution of the JIMWLK evolution equations)

$$\mathcal{W}[x, \rho] = \exp\left\{ - \int dy_\perp dx_\perp \frac{\rho_a(x_\perp) \rho^a(y_\perp)}{2\mu^2(x)} \right\}$$

- $\mu^2(x)$ is the average color charge squared of the valence quarks per unit transverse area and color.

Investigating the CGC

- Cronin Effect at forward rapidities.
- Multiple scatterings of the quark with the nucleus environment ⇒ transverse momentum broadening.

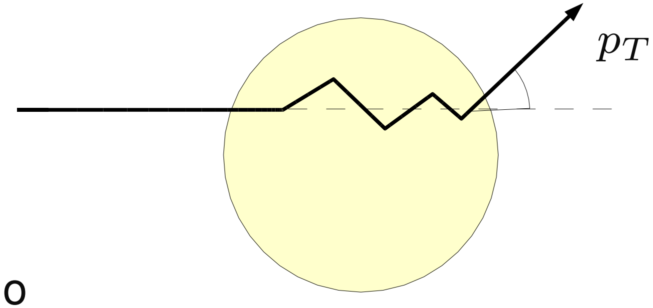

- Nuclear modification ratio

$$R_{dA} = \frac{\frac{d\sigma^{dA \to hX}}{dp_T^2 dy}}{\mathcal{N}_{coll} \frac{d\sigma^{pp \to hX}}{dp_T^2 dy}}$$

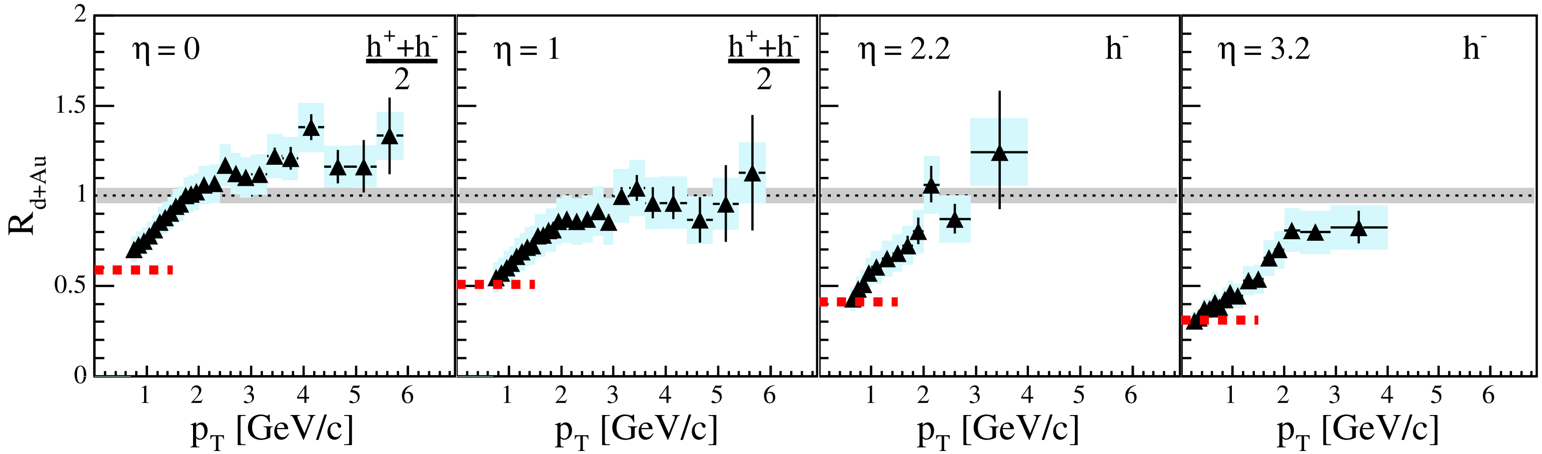

- Central rapidities ⇒ Cronin peak
- Suppression of the ratio with the rapidity;

Cronin effect in the CGC approach

charged hadrons

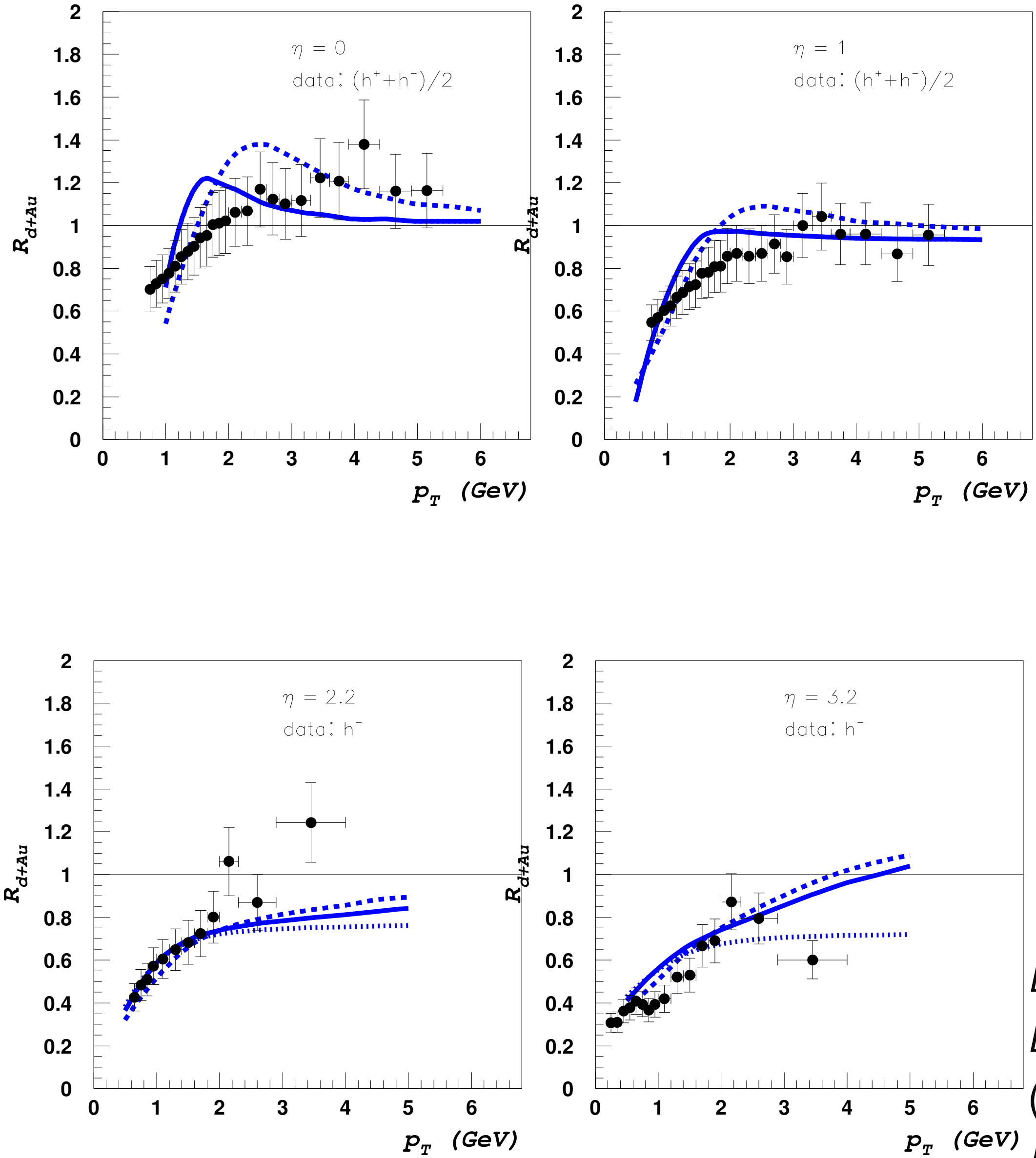

$$R_{dA} = \frac{\frac{d\sigma^{dA\to hX}}{dp_T^2\,dy}}{\mathcal{N}_{coll}\,\frac{d\sigma^{pp\to hX}}{dp_T^2\,dy}}$$

- Data from dA collisions at $\sqrt{s} = 200$ GeV.
- BRAHMS data.
- KKP fragmentation function (*Nucl. Phys. B597, 337 (2001)*)
- dipole-nucleus forward scattering (CGC)
- Consider valence quarks
- Introduce a function to take into account large x gluon behavior
- Suppression at large rapidities $\Rightarrow$ saturation.

D. Kharzeev, Y. V. Kovchegov, K. Tuchin, Phys. Lett. B **599***, 23 (2004).*

(*J. P. Blaizot, F. Gelis and R. Venugopalan, Nucl. Phys. A* **743***, 13 (2004)*)

Dilepton Production in CGC

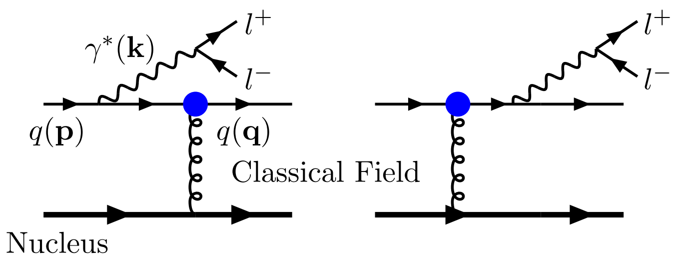

The cross section of dilepton production at forward rapidities can be written as

$$\frac{d\sigma^{pA\to ql^+l^-X}}{dp_T^2\,dM\,dy} = \frac{4\pi^2}{M}R_A^2\frac{\alpha_{em}^2}{3\pi}\int\frac{dl_T}{(2\pi)^3}l_T W(p_T,l_T,x_1)\,C(l_T,x_2,A),$$

- $W(p_T,l_T,x_1)$ analytical calculations $\Rightarrow$ wave function in the momentum space.
- $C(l_T,x_2,A)$ color field correlation $\Rightarrow$ interaction of the quark with the condensated gluonic field (Classical field) $\Rightarrow$ information about the CGC.
- Saturation $\Rightarrow$ low p_T

$$C(l_T)\equiv\int d^2x_\perp e^{il_T\cdot x_\perp}\langle U(0)U^\dagger(x_\perp)\rangle_\rho,$$

- $U(x_\perp)\Rightarrow$ interaction of the quark with the color field of the nucleus.
- Here is where the non-local Gaussian is used to obtain $\langle U(0)U^\dagger(x_\perp)\rangle_\rho$

$$\langle U(0)U^\dagger(x_\perp)\rangle = \int\mathcal{D}_\rho\mathcal{W}_{\Lambda^+}[\rho]U(0)U^\dagger(x_\perp).$$

F. Gelis, J.Jalilian-Marian, Phys. Rev. D **66***, 094014 (2002).*

M.A.Betemps, MBGD, Phys. Rev. D **70***, 116005 (2004). Eur. Phys. J. C* **43***, 365 (2005).*

R. Baier, A. H. Mueller and D. Schiff, Nucl. Phys. A **741***, 358 (2004).*

Nuclear modification ratio

- Investigating the saturation effects,

$$R_{pA} = \frac{\frac{d\sigma(pA)}{R_A^2 dp_T^2 dy dM}}{A^{1/3}\frac{d\sigma(pp)}{R_p^2 dp_T^2 dy dM}}.$$

- Dilepton mass $M = 6$ GeV.
- RHIC energies $\sqrt{s} = 200$ GeV.
- LHC energies $\sqrt{s} = 8800$ GeV.
- Rapidity and p_T spectra.
- Normalization factor $A^{1/3} \Rightarrow$ cylindrical nucleus $\Rightarrow R_A^2$ in the cross section $\Rightarrow R_A^2 \propto A^{2/3}$.

R_{pA} Forward rapidity and p_T

- RHIC $\sqrt{s} = 200$ GeV

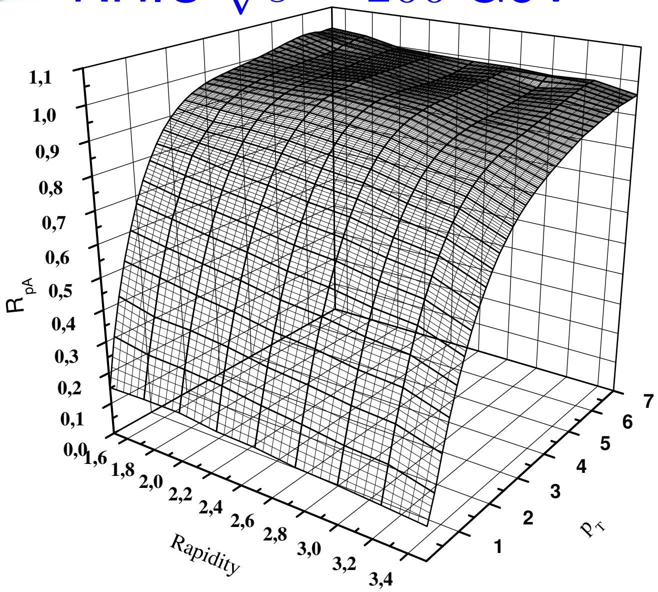

- LHC $\sqrt{s} = 8.8$ TeV

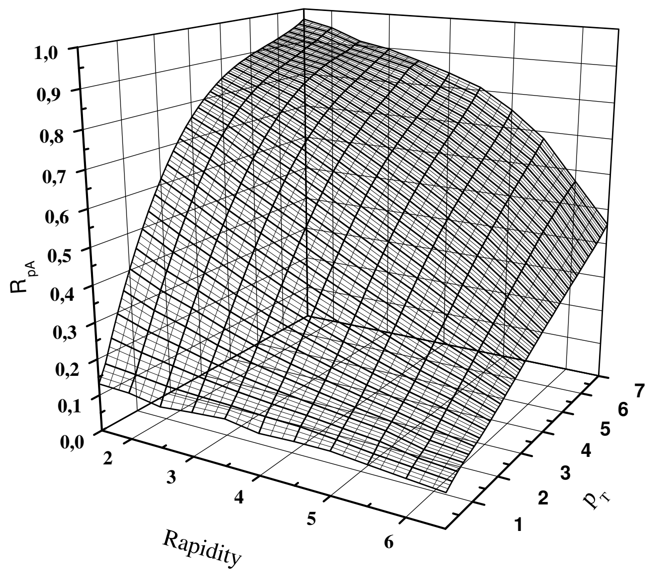

M.A.Betemps, MBGD, Phys. Lett. B, ***636****, 46 (2006).*

- Lepton pair mass $M = 6$ GeV
- Suppression at small p_T;
- Suppression of the Cronin peak;
- RHIC
  - small effects in the rapidity spectra;
  - Effects are independent of the p_T value;
- LHC
  - Suppression in the rapidity spectra is intensified for large p_T;
- Similar behavior of the ratio in p_T at $M = 3$ GeV.

Cronin effect at forward rapidities

- BK/BFKL $\Rightarrow$ suppression of the Cronin peak (suppression at small x for all p_T).

charged hadrons

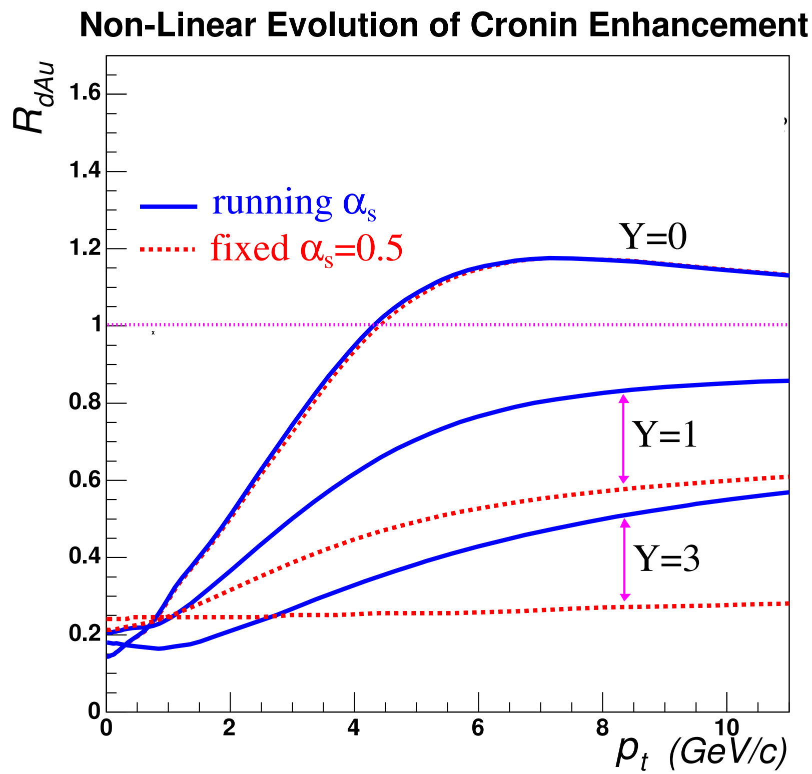

J.V. Albacete et al. Phys. Rev. Lett. **92**, *082001 (2004).*

- Ratio suppression with the rapidity;
- Suppression at forward rapidities $\Rightarrow$ quantum evolution at small x.

Dileptons

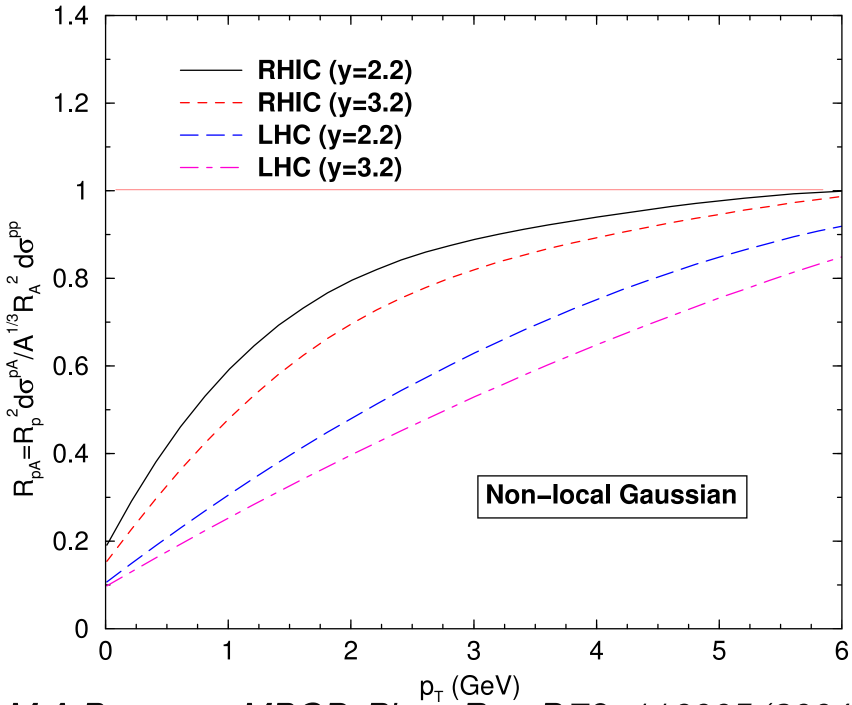

M.A.Betemps, MBGD, Phys. Rev. D **70**, *116005 (2004).*

- Similar behavior of the hadrons;
- Cronin suppression at forward rapidities $\Rightarrow$ Initial state effect;
- Dileptons carry information about the high density QCD system (CGC);

Dilepton at Backward Rapidities

- Dipole picture changing nucleus and proton

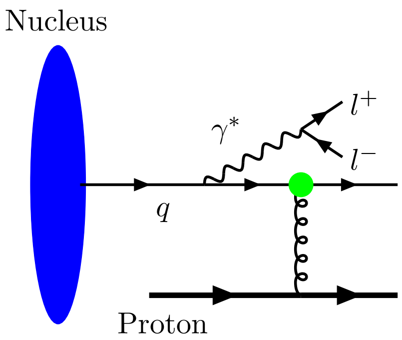

$$\frac{d\sigma^{DY}}{dM^2 dy d^2 p_T} = \frac{\alpha_{em}^2}{6\pi^3 M^2} \int_0^\infty d\rho W(x_2, \rho, p_T) \sigma_{dip}(x_1, \rho),$$

$x_{\binom{1}{2}} = \sqrt{\frac{M^2+p_T^2}{s}} e^{\pm y}$. Large x_2 (nucleus) and small x_1 proton.

$$W(x_2, \rho, p_T) = \int_{x_2}^1 \frac{d\alpha}{\alpha^2} F_2^A(\frac{x_2}{\alpha}, M^2) \left\{ [m_q^2 \alpha^2 + 2M^2(1-\alpha)^2] \left[\frac{1}{p_T^2 + \eta^2} T_1(\rho) - \frac{1}{4\eta} T_2(\rho) \right] \right.$$
$$\left. + [1 + (1-\alpha)^2] \left[\frac{\eta p_T}{p_T^2 + \eta^2} T_3(\rho) - \frac{1}{2} T_1(\rho) + \frac{\eta}{4} T_2(\rho) \right] \right\},$$

$\alpha \Rightarrow$ momentum fraction of the quark carried by the virtual photon

$$T_1(\rho) = \frac{\rho}{\alpha} J_0(\frac{p_T \rho}{\alpha}) K_0(\frac{\eta\rho}{\alpha})$$
$$T_2(\rho) = \frac{\rho^2}{\alpha^2} J_0(\frac{p_T \rho}{\alpha}) K_1(\frac{\eta\rho}{\alpha}) \qquad (\eta^2 = (1-\alpha)M^2 + \alpha^2 m_q^2)$$
$$T_3(\rho) = \frac{\rho}{\alpha} J_1(\frac{p_T \rho}{\alpha}) K_1(\frac{\eta\rho}{\alpha}).$$

M.A. Betemps, MBGD, E.G. de Oliveira, hep-ph/0607247.

Coherence length (l_c) at backward

- mean lifetime of fluctuation $|ql^+l^-\rangle$.
- Important quantity controlling $\Rightarrow$ nuclear effects.
- l_c smaller than the target (Fig (a)) $\Rightarrow$ energy loss in the target (there is no significative energy loss with proton target).
- l_c larger than the target (Fig (b)) $\Rightarrow$ cross section in the factorized form

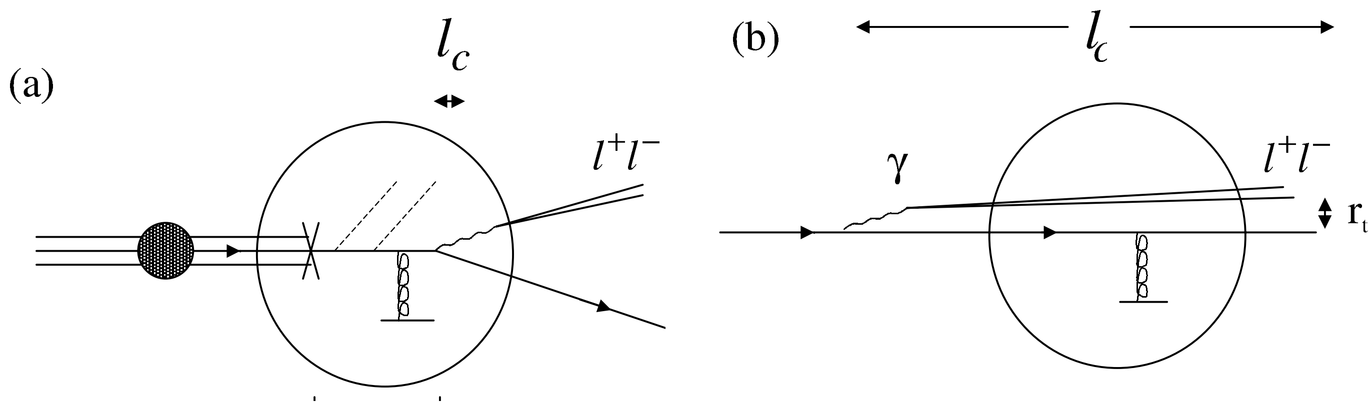

M.B.Johnson, et al. Phys. Rev. Lett. **86**, *4483 (2001).*

l_c at backward (our case - insight for backward)

- Consider here large $l_c \propto \frac{1}{x_1} \Rightarrow x_1$ momentum fraction of the proton target.
- Applicable only at small x_1 (proton).
- Explain the exchange between proton and nucleus in the dipole approach.

Nuclear parton distributions and σ_{dip}

- Eskola, Kolhinen and Salgado (EKS parametrization) *Eur. Phys. J. C* **9**, *61 (1999)*
- D. de Florian and R. Sassot (nDS parametrization) *Phys. Rev. D* **69**, *074028 (2004)*

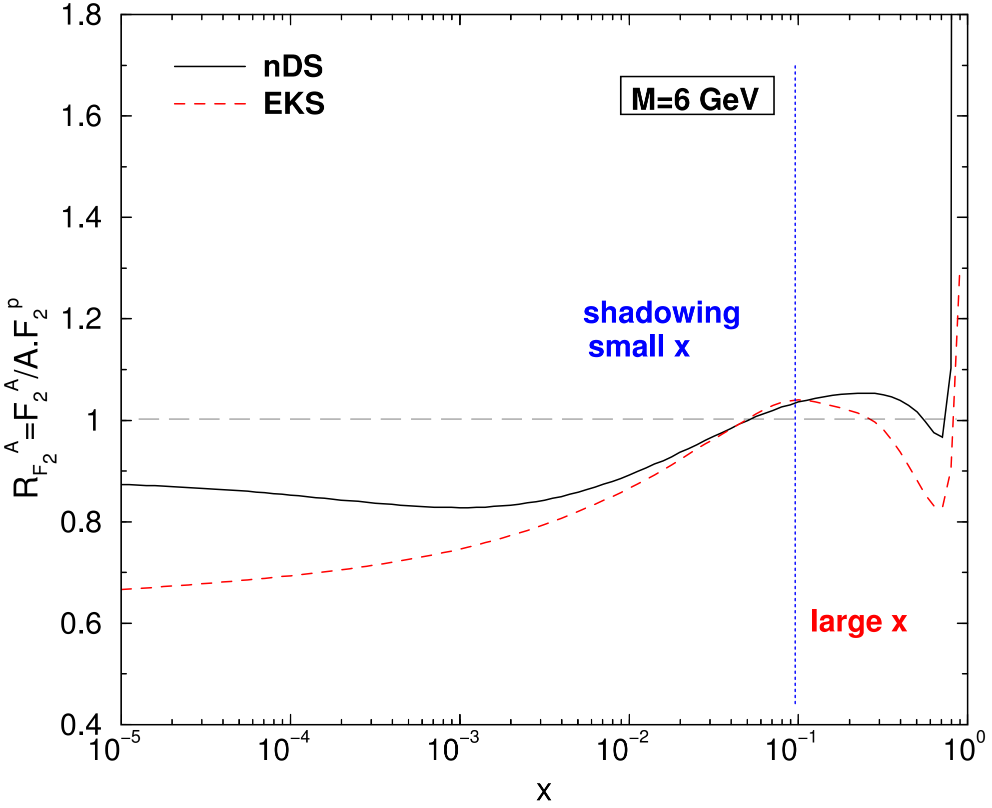

- $\sigma_{dip} \Rightarrow$ GBW dipole cross section $\sigma_{dip}(x,r) = \sigma_0 (1 - \exp\left\{ \left(\frac{r^2 Q_0^2}{4(x/x_0)^{\lambda}} \right) \right\}$
- Fit to the HERA data ($\sigma_0 = 23.03$mb, $x_0 = 3.04 \times 10^{-4}$, $\lambda = 0.288$)
  K. Golec-Biernat, M. Wusthoff, Phys. Rev. D **59**, *014017 (1999)*

Nuclear modification ratio

- Investigating effects in the backward region,

$$R_{pA} = \frac{\frac{d\sigma(pA)}{dp_T^2 dy dM}}{A \frac{d\sigma(pp)}{dp_T^2 dy dM}}.$$

- Dilepton mass $M = 6$ GeV.
- RHIC energies $\sqrt{s} = 200$GeV.
- LHC energies $\sqrt{s} = 8800$ GeV.
- Rapidity and p_T spectra.
- Normalization factor $A \Rightarrow$ nucleus configuration $\rightarrow$ there is no R_A^2 in the cross section.

Backward rapidity and p_T at RHIC

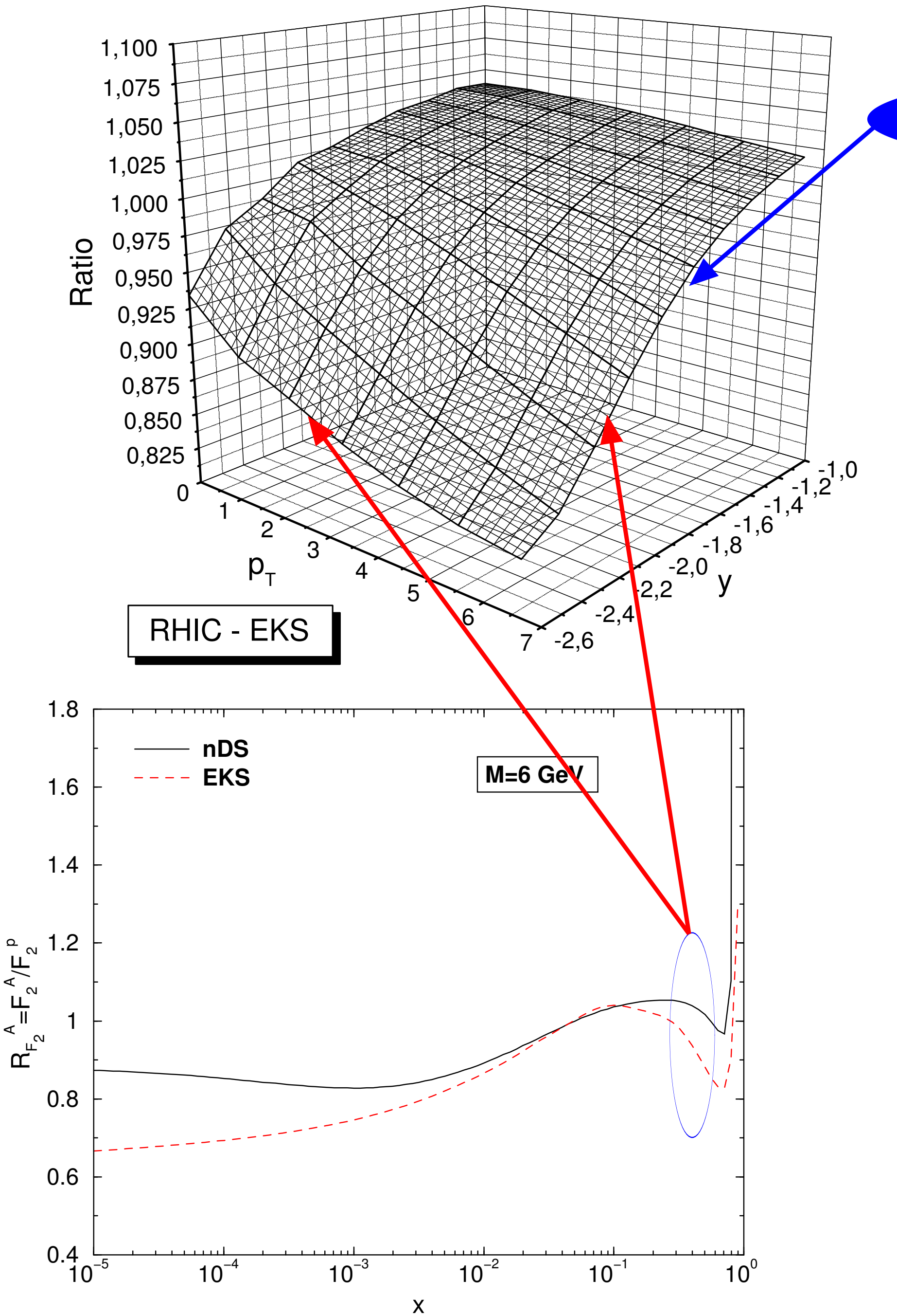

- $0.08 < x_2 < 0.5$.
- Large x nuclear effect;
- lower $y \rightarrow$ large x_2
- Suppression in $y \rightarrow$ large x effect;
- large $p_T \rightarrow$ large x_2;
- Suppression in $p_T \rightarrow$ large x effect $\rightarrow$ less intense;
- Comparison EKS $\times$ nDS (large x effect predictions).

Backward rapidity and p_T at LHC

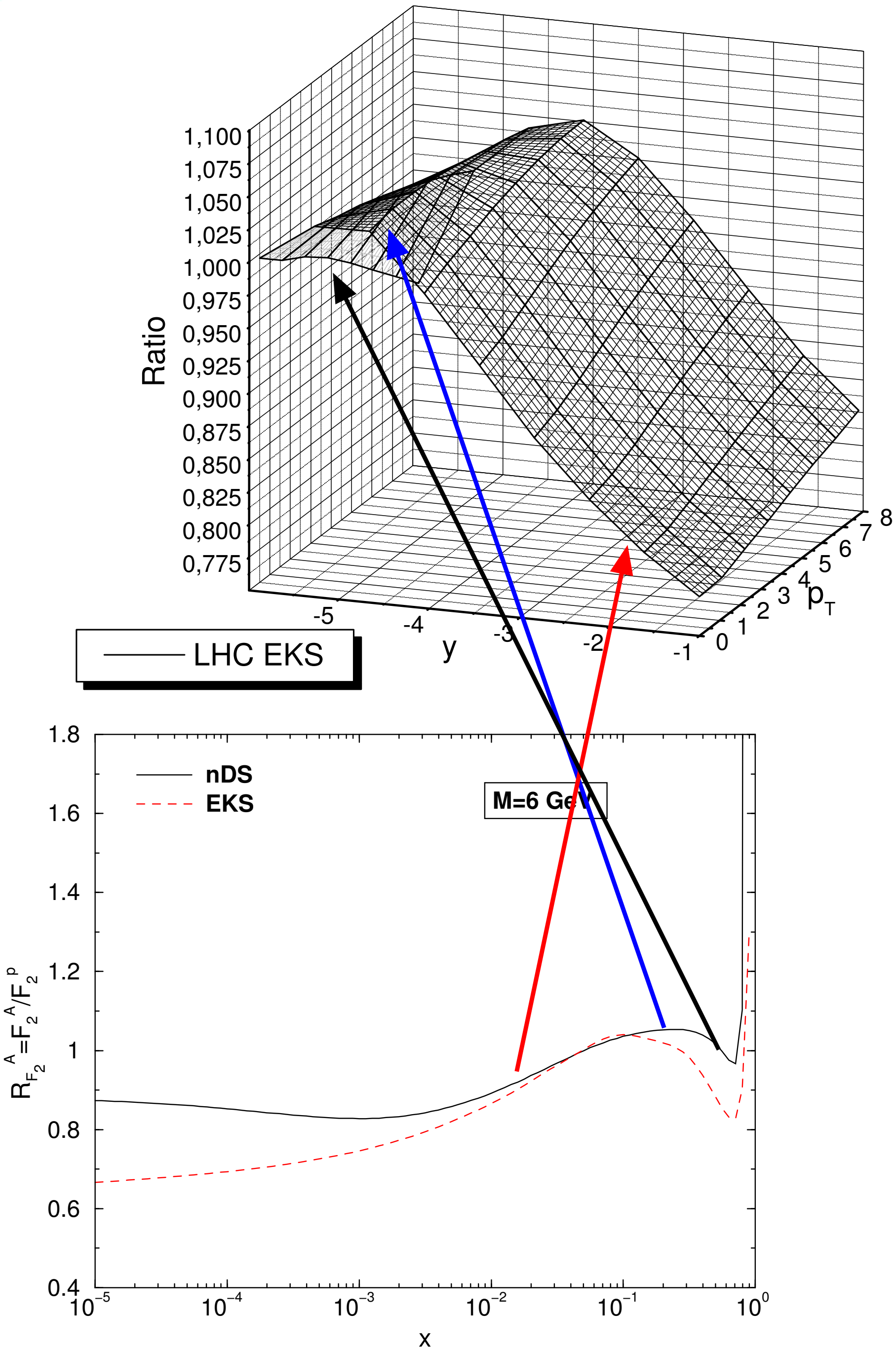

- $0.002 < x_2 < 0.3$.
- antishadowing and shadowing nuclear effects;
- Peak at $y \sim -4.5 \rightarrow$ antishadowing effect;
- Two behaviors with p_T:
  - Suppression in $p_T \rightarrow$ large x effect (very backward);
  - Decreasing with $p_T \rightarrow$ shadowing effect;
- EKS $\times$ nDS (similar behavior)
- Caution with the terminology (pdf's).

Dilepton at backward-forward rapidities

- RHIC energies.

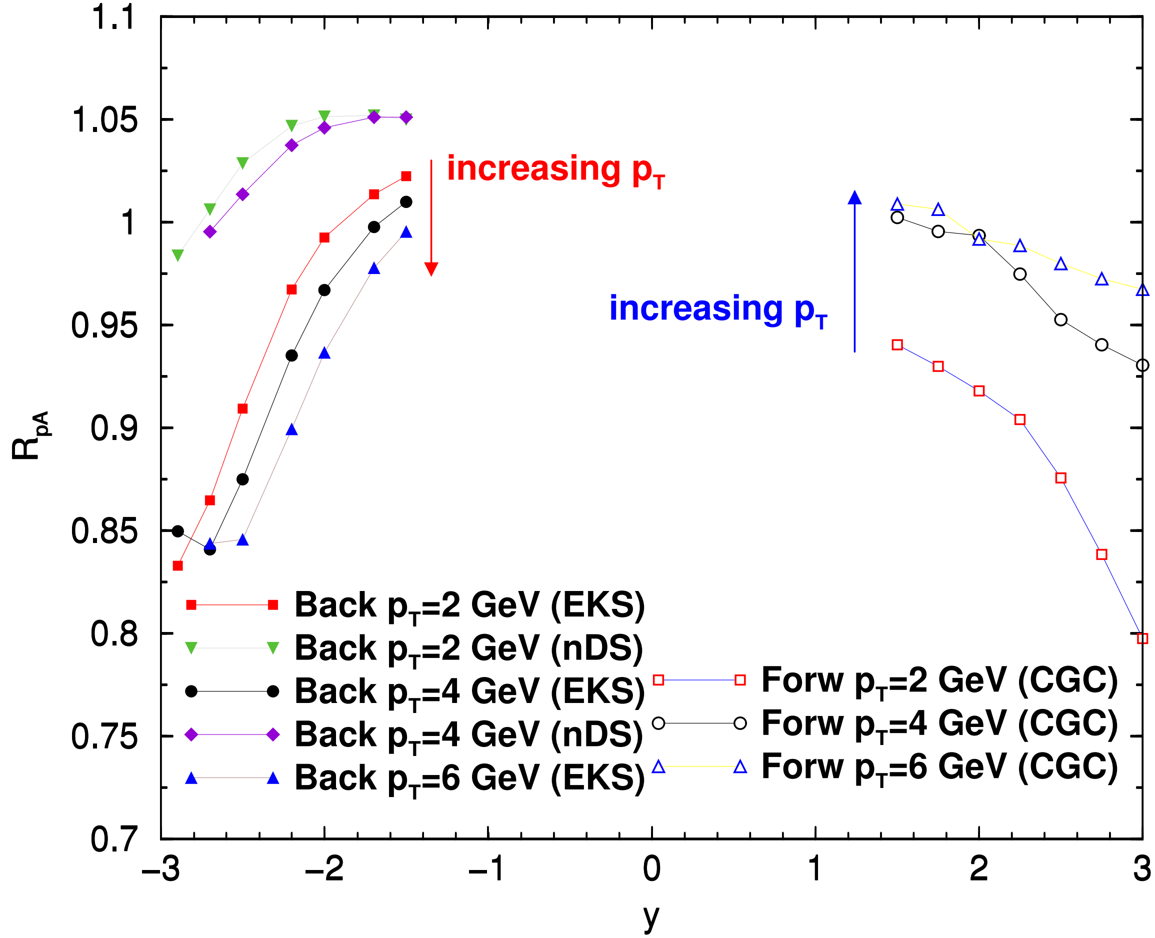

- $R_{pA} \Rightarrow$ Different p_T behavior.

$$\begin{cases} \text{Forward} \Rightarrow p_T \text{ increases} \Rightarrow R_{pA} \text{ enlarged (saturation)} \\ \text{Backward} \Rightarrow p_T \text{ increases} \Rightarrow R_{pA} \text{ reduced (large } x \text{ effects)} \end{cases}$$

Cronin at backward-forward rapidities

- Hadrons

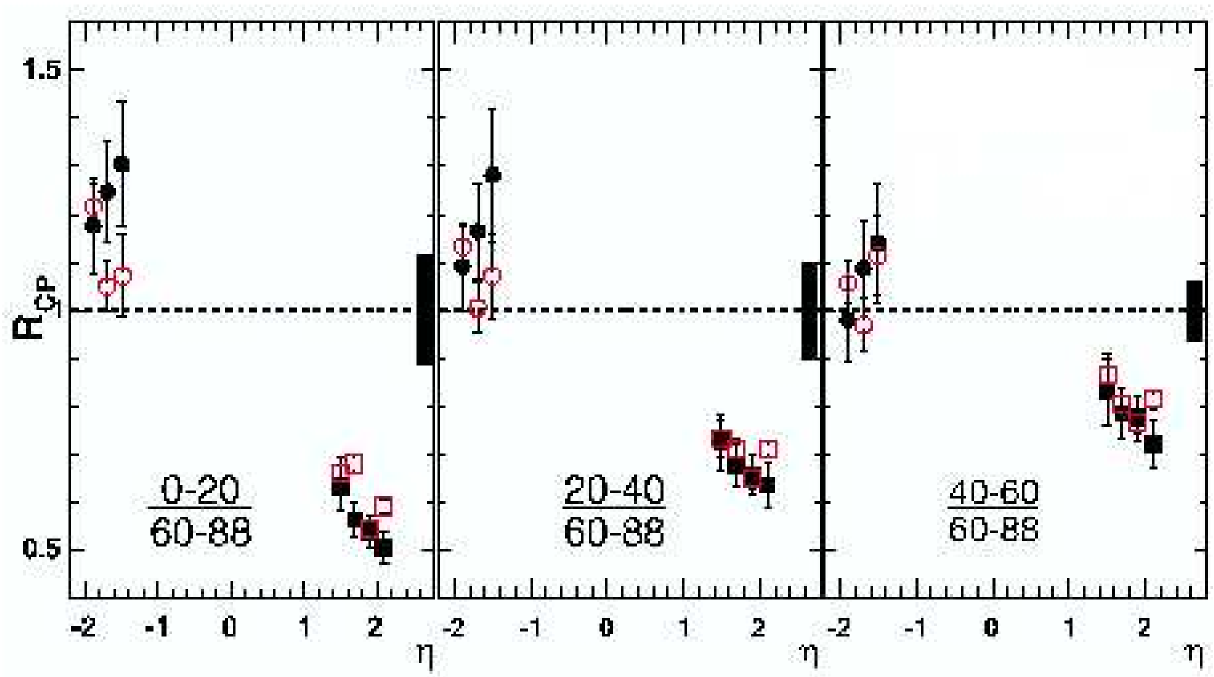

- Pronounced peak at backward rapidities (0.5 GeV $< p_T <$ 4 GeV).
- R_{pA} for dileptons prediction for RHIC does not present such a peak.
- Cronin peak at backward rapidities at RHIC energies $\Rightarrow$ large x effects + final state effect.

S.S. Adler, et al. PHENIX *Collaboration, Phys. Rev. Lett.* **94**, *082302 (2005).*

Dilepton × Hadrons

R_{pA}	Forward	Backward
Dileptons	- Suppression of Cronin peak. - Saturation	**Rapidity Spectra** - Weak enhancement of R_{pA} in comparison with forward. - (RHIC) - Large x nuclear effects. - (LHC) - Large and small x nuclear effects. **Transverse Momentum** (RHIC) - R_{pA} reduces as p_T increases (large x effects) (LHC) - two behaviors (small and large x effects)
Hadrons	- Suppression of Cronin peak. - Saturation - Initial state effect.	- Enhanced Cronin peak in the rapidity spectra in comparison with forward (DATA). - Large x nuclear effects + final state effects (Dileptons indicate that).

Conclusions

- Saturation effects should be present at RHIC, hadrons and dileptons, at forward rapidities.
- Nuclear modification ratio suppression at forward rapidities for dileptons indicates the Cronin suppression for hadrons as initial state effect.
- At backward rapidities dileptons present different p_T dependence at RHIC (large x nuclear effects) comparing with the forward ones (saturation) (non symmetric).
- At LHC energies and backward rapidities, the p_T distribution for the ratio R_{pA} present distinct behaviors comparing very backward (large x effects) and more central rapidities (shadowing).
- Cronin effect peak in the rapidity spectra for hadrons at backward rapidities should be due to $\Rightarrow$ final state effects + large x nuclear effects.